

Short Seeking by Multi-rate Digital Controllers for Computation Saving with Initial Value Adjustment

Li Yang and Masayoshi Tomizuka

Department of Mechanical Engineering

University of California at Berkeley

Berkeley, California 94720, U.S.A.

yangli@me.berkeley.edu , tomizuka@me.berkeley.edu

Abstract

Multi-rate control has been proposed to reduce the real time computation in hard disk drive servo systems. It has been showed that computation can be saved greatly without performance degradation by using multi-rate controller for track following. In this report, we propose a novel method for short seeking control based on multi-rate track following control and initial value adjustment for both single-actuator HDDs and dual-actuator HDDs.

The proposed method, which utilizes the same multi-rate controller and same servo structure as track following, adjusts the initial values of the track-following controller for short seeking. Real time computation is greatly saved in two aspects: first, computation is saved by multi-rate scheme; second, initial value adjustment of the feedback controller makes the use of the feed-forward controller and reference trajectory unnecessary.

Simulation and experimental results confirmed that an excellent short-seeking performance can be achieved with a small amount of real time computation using the proposed methods for both single-actuator HDDs and dual-actuator HDDs.

Keywords—Multi-rate control, Short seeking, Hard disk drives, Dual stage

1. Introduction

Recently, multi-rate control has been proposed as a solution to reduce the real time computation in hard disk drive servo systems. In the implementation of servo systems for HDDs with digital control, the amount of computation for real time control is a big concern. The HDD industry strives for lowering cost and the control algorithm must be implemented on a low end DSP, which may be performing various other tasks, and large amount of computation may overload the DSP. Multi-rate scheme reduces real time computation by updating different components of the controller at different rates, i.e. slow components of the controller can be updated less frequently to reduce the computation load. It has been shown that this scheme greatly saves computation without performance degradation in the implementation of the track following controller [1].

Short seeking control is for moving the read/write head across a few tracks to the target track quickly and precisely. Short seeking control may be based on a two-degree-of-freedom (TDOF) servo structure, which requires the design and implementation of both the feed-forward controller and reference trajectory [2]-[5]. Because of extra real time computation for feed-forward control, the amount of computation is larger in TDOF short seeking control than in tracking following control. Hirata and Tomizuka avoided the use of the TDOF structure in short seeking by adjusting the initial value of the feedback controller [6].

In this report, we propose a novel method for short seeking control based on multi-rate track following control [1] and initial value adjustment. This method, which uses the same multi-rate controller and same servo structure as track following, tunes the initial values of the track-following controller for short seeking. The proposed method significantly saves real time computation in two aspects: first, multi-rate scheme inherently saves computation by updating the slow-component controller at slow rate; second, by tuning the initial values of the feedback controller, the desired transient characteristics in short-seeking can be obtained without the use of feed-forward controller, which implies no real time computation for feed-forward control is needed.

The remainder of this report is organized as follows. In Section 2, the multi-rate short seeking control with initial value adjustment is proposed for single-actuator HDDs. In Section 3, the multi-rate short seeking control with initial value adjustment is proposed for dual-actuator HDDs. In Section 4, the proposed methods are applied to a HDD, and the simulation results and experiment results are given. Conclusions are given in Section 5.

2. Multi-rate Short Seeking Control with Initial Value Adjustment for single-actuator HDDs

2.1 Overall Control Structure for Short Seeking

Fig. 1 shows a schematic diagram of proposed short seeking control by initial value adjustment of multi-rate track-following controller for HDDs. P represents the dynamics of the plant. $C(z)$ is a track following controller and it can be separated into a slow-mode controller C_s and a fast-mode controller C_f [1]:

$$C(z) = C_s(z) + C_f(z)$$

D and I are the decimator and the interpolator respectively. The proposed system has the following features:

- (1) The overall structure during seeking is a one-degree-of-freedom (ODOF) structure.
- (2) Reference input is set to be a step signal for short seeking, i.e., $r(k)=r$ for $k \geq 0$, where r is the seeking distance. The output signal is sampled with period T_f .
- (3) The multi-rate feedback controller is the same as the track following controller. The fast-mode component of the controller C_f is updated at the measurement sampling rate ($1/T_f$), while the slow-mode component C_s is updated m times slower than the measurement sampling rate with period $T_s = mT_f$. The multi-rate ratio m is an integer greater than 1.
- (4) Nonzero initial values are set to both the slow-mode controller and the fast-mode controller for short seeking.

Notice that the adjustment of the initial values of the controller improves the transient response without changing closed-loop characteristics such as stability and sensitivity. Since we already have the design methodology for multi-rate track following controllers [1], finding the initial values of the multi-rate controllers becomes the main issue. A methodology on how to find the optimal initial values of the multi-rate controller is presented in this report. In the following sub-section 2.2, the multi-rate short seeking control problem is formulated as an optimization problem by converting the multi-rate control system depicted in Fig.1 to an equivalent MIMO single-rate system. Then in sub-section 2.3, the optimal initial values of the controller for the equivalent MIMO system are sought to minimize the performance index based on the tracking error. Design of performance index for short-seeking is discussed in sub-section 2.4.

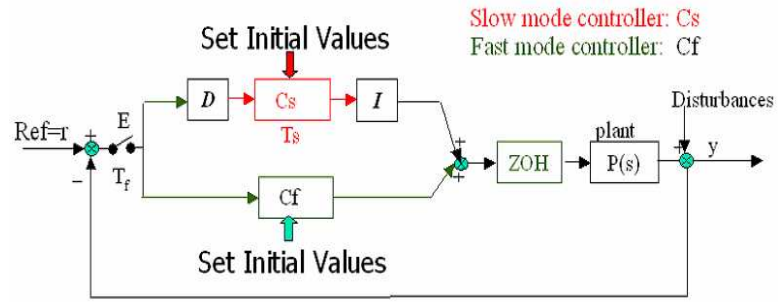


Fig. 1 Schematic diagram of multi-rate short-peek control with IVA for HDDs

2.2 Representation of the Multi-rate Control System a Single-rate system via Lifting

Assume that the dynamic model of the plant in continuous time is

$$\begin{aligned}\dot{x}_v(t) &= A_0 x_v(t) + B_0 u(t) \\ y(t) &= C_0 x_v(t)\end{aligned}\quad (1)$$

where $x_v(t)$ is a n_v th-order state vector of the plant, $u(t), y(t)$ are the control input and measurement output, and A_0, B_0, C_0 are $n_v \times n_v, n_v \times 1, 1 \times n_v$ real matrices, respectively.

The discrete time equivalent of (1) with measurement sampling period T_f is expressed by

$$\begin{aligned}x_v((k+1)T_f) &= A_1 x_v(kT_f) + B_1 u(kT_f) \\ y(kT_f) &= C_1 x_v(kT_f)\end{aligned}\quad (2)$$

where

$$A_1 = e^{A_0 T_f}, \quad B_1 = \int_0^{T_f} e^{A_0 t} B_0 dt, \quad C_1 = C_0 \quad (3)$$

Suppose a track following controller has already been designed to meet performance specifications for the plant, so that the closed loop system is stable and steady state error is zero. As an example, we consider a third order digital controller with two slow modes and one fast mode given by

$$C(z) = \frac{b_1}{z-a_1} + \frac{b_2}{z-a_2} + \frac{b_3}{z-a_3} + d_3 = C_s(z) + C_f(z) \quad (4)$$

$$\text{where } C_s(z) = \frac{b_1}{z-a_1} + \frac{b_2}{z-a_2}, C_f(z) = \frac{b_3}{z-a_3} + d_3 \quad (5)$$

Referring to Fig. 1, the slow-mode controller $C_s(z)$ is updated m times slower than the fast-mode controller $C_f(z)$. The controller $C(z)$ cannot be described in the standard state-space form because it is a time-periodic system. Thus, we introduce a discrete-time lifting technique to describe the multi-rate system by an equivalent single-rate system, which may be accomplished in the following three steps.

STEP 1) *The multi-rate controller in the transfer domain is transformed to an equivalent MIMO single-rate controller in the time domain with slow period T_s .*

Lemma 1: Under the proposed multi-rate implementation scheme, the controller described by Eq.(4) can be represented by a MIMO single-rate system in time domain as following:

$$\begin{aligned} x_c[k+1] &= A_c x_c[k] + B_c \bar{e}[k] \\ \bar{U}[k] &= C_c x_c[k] + D_c \bar{e}[k] \end{aligned} \quad (6)$$

where $x_c[k]$ is a 3rd-order state vector of the controller and $\bar{e}[k], \bar{U}[k]$ are the lifted position error signal and lifted control signal:

$$x_c[k] := x_c(kT_s) \quad (7)$$

$$\bar{e}[k] = \begin{bmatrix} e[k,0] \\ e[k,1] \\ \dots \\ e[k,m-1] \end{bmatrix} = \begin{bmatrix} e(kT_s) \\ e(kT_s + T_f) \\ \dots \\ e(kT_s + (m-1)T_f) \end{bmatrix} \quad (8)$$

$$\bar{U}[k] = \begin{bmatrix} u[k,0] \\ u[k,1] \\ \dots \\ u[k,m-1] \end{bmatrix} = \begin{bmatrix} u(kT_s) \\ u(kT_s + T_f) \\ \dots \\ u(kT_s + (m-1)T_f) \end{bmatrix} \quad (9)$$

$A_c \in \Re^{3 \times 3}$, $B_c \in \Re^{3 \times m}$, $C_c \in \Re^{m \times 3}$ and $D_c \in \Re^{m \times m}$ are:

$$A_c = \begin{bmatrix} a_1^m & 0 & 0 \\ 0 & a_2^m & 0 \\ 0 & 0 & a_3^m \end{bmatrix}, B_C = \begin{bmatrix} \sum_{i=0}^{m-1} a_1^i b_1 & 0 & \dots & 0 \\ \sum_{i=0}^{m-1} a_2^i b_2 & 0 & \dots & 0 \\ a_3^{m-1} b_3 & a_3^{m-2} b_3 & \dots & b_3 \end{bmatrix}, C_c = \begin{bmatrix} 1 & 1 & 1 \\ 1 & 1 & a_3 \\ 1 & 1 & a_3^2 \\ \dots \\ 1 & 1 & a_3^{m-1} \end{bmatrix}, D_c = \begin{bmatrix} d_3 & & & & \\ b_3 & d_3 & & & \\ a_3 b_3 & b_3 & d_3 & & \\ \dots & & & & \\ a_3^{m-2} b_3 & a_3^{m-3} b_3 & \dots & b_3 & d_3 \end{bmatrix} \quad (10)$$

Proof:

Note that $C(z)$ can be expressed in the time domain as

$$\begin{bmatrix} x_1(k+1) \\ x_2(k+1) \\ x_3(k+1) \end{bmatrix} = \begin{bmatrix} a_1 & 0 & 0 \\ 0 & a_2 & 0 \\ 0 & 0 & a_3 \end{bmatrix} \begin{bmatrix} x_1(k) \\ x_2(k) \\ x_3(k) \end{bmatrix} + \begin{bmatrix} b_1 \\ b_2 \\ b_3 \end{bmatrix} e(k) \quad (11)$$

$$u(k) = [1 \quad 1 \quad 1]x(k) + d_3 e(k) \quad (12)$$

where $x_c(k) := [x_1(k) \quad x_2(k) \quad x_3(k)]' = x_c(kT_f)$

Under the proposed multi-rate scheme, x_3 corresponds to fast mode, and is updated at fast rate ($1/T_f$), so

$$\begin{aligned} x_3[(k+1)T_s] &= x_3(kT_s + mT_f) \\ &= a_3 x_3(kT_s + (m-1)T_f) + b_3 e(kT_s + (m-1)T_f) \\ &= a_3 [a_3 x_3(kT_s + (m-2)T_f) + b_3 e(kT_s + (m-2)T_f)] \\ &\quad + b_3 e(kT_s + (m-1)T_f) \\ &= a_3^2 x_3(kT_s + (m-2)T_f) + a_3 b_3 e(kT_s + (m-2)T_f) \\ &\quad + b_3 e(kT_s + (m-1)T_f) \\ &\dots \\ &= a_3^m x_3(kT_s) + \sum_{i=0}^{m-1} a_3^{m-1-i} b_3 e(kT_s + iT_f) \end{aligned} \quad (13)$$

x_1 and x_2 correspond to slow modes, and are updated at slow rate ($1/T_s$), so the input to the controller is held constant during one slow period T_s , i.e.

$$e(kT_s) = e(kT_s + iT_f) \quad \text{for } i = 0, 1, \dots, m-1 \quad (14)$$

$$\text{Thus, } x_1[(k+1)T_s] = a_1^m x_1(kT_s) + \sum_{i=0}^{m-1} a_1^i b_1 e(kT_s) \quad (15)$$

$$x_2[(k+1)T_s] = a_2^m x_2(kT_s) + \sum_{i=0}^{m-1} a_2^i b_2 e(kT_s) \quad (16)$$

Furthermore, from state equation (12), we obtain

$$u(kT_s) = x_1(kT_s) + x_2(kT_s) + x_3(kT_s) + d_3 e(kT_s) \quad (17)$$

and by noting $x_1(kT_s + iT_f) = x_1(kT_s)$, $x_2(kT_s + iT_f) = x_2(kT_s)$ for $i=1, 2, \dots, m-1$, we obtain

$$\begin{aligned} u(kT_s + iT_f) &= x_1(kT_s) + x_2(kT_s) + x_3(kT_s + iT_f) + d_3 e(kT_s + iT_f) \\ &= x_1(kT_s) + x_2(kT_s) + d_3^i x_3(kT_s) \\ &\quad + \sum_{j=0}^{i-1} d_3^{i-1-j} b_3 e(kT_s + jT_f) + d_3 e(kT_s + iT_f) \end{aligned} \quad (18)$$

Since x_1 and x_2 are updated slower than x_3 , we can introduce a discrete-time lifting technique to describe the multi-rate controller in terms of the lifted error signal (8) and the lifted control signal (9).

Combining Eqs. (15), (16), (13), (17) and (18), and using (8) and (9), we can represent the controller as a time-invariant system with the slow update period T_s as follows:

$$\begin{aligned} x_c[k+1] &= A_c x_c[k] + B_c \bar{e}[k] \\ \bar{U}[k] &= C_c x_c[k] + D_c \bar{e}[k] \end{aligned}$$

where $x_c[k] = [x_1[k] \ x_2[k] \ x_3[k]]' = x_c(kT_s)$, and matrices A_c, B_c, C_c and D_c are as defined in (10). □

STEP 2) The plant is expressed by an equivalent MIMO single-rate plant in the time domain with the underlying slow period T_s .

The plant described by Eq. (2) can also be expressed by an equivalent MIMO single-rate plant given by

$$\begin{aligned} x_v[k+1] &= A_v x_v[k] + B_v \bar{U}[k] \\ \bar{Y}[k] &= C_v x_v[k] + D_v \bar{U}[k] \end{aligned} \quad (20)$$

where

$$x_v[k] = x_v(kT_s),$$

$$\bar{Y} = \begin{bmatrix} y[k,0] \\ y[k,1] \\ \dots \\ y[k,m-1] \end{bmatrix} = \begin{bmatrix} y(kT_s) \\ y(kT_s + T_f) \\ \dots \\ y(kT_s + (m-1)T_f) \end{bmatrix},$$

$$A_v = A_1^m, \quad B_v = [A_1^{m-1} B_1, A_1^{m-2} B, \dots, B_1], \quad C_v = \begin{bmatrix} C_1 \\ C_1 A_1 \\ \dots \\ C_1 A_1^{m-1} \end{bmatrix} \quad (21)$$

STEP 3) Combining the controller and plant equations from STEP 1 and 2, we obtain a MIMO single-rate representation of the closed loop system in lifted form.

From the controller equation (6) and plant equation (20), we obtain the closed loop system:

$$\begin{aligned} x[k+1] &= Ax[k] + B\bar{r} \\ \bar{Y}[k] &= Cx[k] + D\bar{r} \end{aligned} \quad (22)$$

where

$$\begin{aligned} x[k] &:= \begin{bmatrix} x_v[k] \\ x_c[k] \end{bmatrix} \in \mathfrak{R}^{n_v+3}, \quad \bar{r} = \begin{bmatrix} r \\ r \\ \dots \\ r \end{bmatrix} \in \mathfrak{R}^m, \\ A &= \left\{ \begin{bmatrix} A_v & B_v C_c \\ 0 & A_c \end{bmatrix} - \begin{bmatrix} B_v D_c \\ B_c \end{bmatrix} [I + D_v D_c]^{-1} \begin{bmatrix} C_v & D_v C_c \end{bmatrix} \right\}, \\ B &= \begin{bmatrix} B_v D_c \\ B_c \end{bmatrix} [I + D_v D_c]^{-1}, \quad C = [I + D_v D_c]^{-1} \begin{bmatrix} C_v & D_v C_c \end{bmatrix}, \\ D &= [I + D_v D_c]^{-1} D_v D_c \end{aligned} \quad (23)$$

Now the multi-rate control system Fig 1 is converted to an equivalent MIMO single-rate system described by (22). The lifted system equivalent to the multi-rate short-seeking control system is shown in Fig. 2.

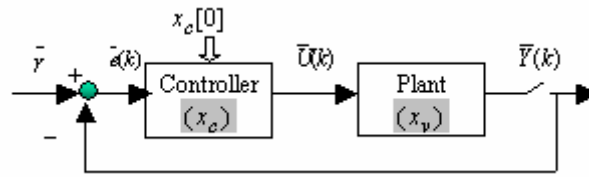


Fig. 2 Lifted system equivalent to the multi-rate short-seeking control system

The resulting closed loop system (22) is asymptotically stable because the multi-rate track following controller has been designed to stabilize the system. The error dynamics of the closed loop system is:

$$e_x[k+1] = Ae_x[k] \quad (24)$$

$$\text{where } e_x[k] = x[k] - x[\infty], \quad x[\infty] = (I - A)^{-1} B\bar{r} \quad (25)$$

2.3 Initial Value Adjustment of the Multi-rate Controller

After the multi-rate control system is converted to an equivalent MIMO single-rate system, the initial value adjustment of the multi-rate controller can be formulated as the following optimization problem.

Problem 1: Consider the multi-rate control system depicted in Fig. 1 or the equivalent MIMO single-rate system described by equation (22). Find the initial value of the controller $x_c[0]$ that minimizes performance index J :

$$J = \sum_{k=0}^{\infty} e_x[k]^T Q e_x[k], \text{ for } Q > 0 \quad (26)$$

where $e_x[k]$ is as defined in (25).

Theorem 1: The initial value of the controller $x_c[0]$ that minimizes performance index J is:

$$x_c[0] = K \bar{r} \quad (27)$$

$$\text{where } K = \begin{bmatrix} P_{cc}^{-1} P_{vc}^T & I \end{bmatrix} (I-A)^{-1} B \quad (28)$$

and P_{cc}, P_{vc} are obtained by solving the Lyapunov equation:

$$A^T P A - P = -Q, \quad P = \begin{bmatrix} P_{vv} & P_{vc} \\ P_{vc}^T & P_{cc} \end{bmatrix} \quad (29)$$

Proof: Since A is asymptotically stable, (29) has a unique positive definite solution $P > 0$, and the performance index J can be transformed to

$$J = e_x[0]^T P e_x[0] \quad (30)$$

where

$$e_x[0] = \begin{bmatrix} x_v[0] \\ x_c[0] \end{bmatrix} - x[\infty] = \begin{bmatrix} e_{xv}[0] \\ e_{xc}[0] \end{bmatrix} \quad (31)$$

It is easy to show that $\partial J / \partial x_c[0] = 0$ is equivalent to:

$$\frac{\partial J}{\partial e_{xc}(0)} = 0 \quad (32)$$

Further, from (30) and (31)

$$J = e_{xv}^T[0] P_{vv} e_{xv}[0] + 2e_{xv}^T[0] P_{vc} e_{xc}[0] + e_{xc}^T[0] P_{cc} e_{xc}[0] \text{ Solving } \partial J / \partial e_{xc}(0) = 0, \text{ we get}$$

$$e_{xc}(0) = -P_{cc}^{-1} P_{vc}^T e_{xv}(0) \quad (33)$$

From (31) and (33), and noting that $x_v[0]$ may be assumed zero for short seeking, we conclude that J is minimized for $x_c[0] = K \bar{r}$, where $K = [P_{cc}^{-1} P_{vc}^T \quad I](I-A)^{-1} B$

From (27) and (28), we note that the initial value of the controller $x_c[0]$ is determined by \bar{r} , A , B and P . We further note that \bar{r} is determined by r (see E.q. (23)) and P is determined by Q and A (see E.q. (29)). Thus, given, Q , r , A and B , the initial value of the controller $x_c[0]$ can be computed off-line.

2.4 Design of Performance Index Function

The performance index J plays an important role in determining the initial value of the controller and thus the seeking performance. To obtain good performance in short seeking, the performance index is based on the squared summation of the tracking error and smoothness of the control input for enhanced performance:

$$J = J_1 + qJ_2 \quad (34)$$

$$\text{where } J_1 = \sum_{k=0}^{\infty} [\bar{Y}(k) - \bar{Y}(\infty)]^T [\bar{Y}(k) - \bar{Y}(\infty)], \quad J_2 = \sum_{k=0}^{\infty} [\bar{U}(k) - \bar{U}(\infty)]^T [\bar{U}(k) - \bar{U}(\infty)] \quad (35)$$

and q is a weighting factor.

Lemma 2: The performance index J in (34) can be transformed into the standard quadratic form:

$$J = \sum_{k=0}^{\infty} e_x[k]^T Q e_x[k]$$

$$\text{where } Q = C^T C + q C_u^T C_u, \quad C_u = (I + D_c D_v)^{-1} [-D_c C_v, C_c] \quad (36)$$

Proof:

From (6), it is easy to show:

$$\bar{U}[k] = C_c x_c[k] + D_c \bar{e}[k] = C_c x_c[k] + D_c (\bar{r} - \bar{Y}[k]) \quad (37)$$

By substituting $\bar{Y}[k] = C_v x_v[k] + D_v \bar{U}[k]$ into (37), we get

$$\bar{U}[k] = (I + D_c D_v)^{-1} [-D_c C_v, C_c] x[k] + (I + D_c D_v)^{-1} D_c \bar{r} = C_u x[k] + D_u \bar{r}$$

where $C_u = (I + D_c D_v)^{-1} [-D_c C_v, C_c]$,

$$D_u = (I + D_c D_v)^{-1} D_c$$

Thus, $\bar{U}(k) - \bar{U}(\infty) = C_u [x(k) - x(\infty)] = C_u e_x(k)$

Also, $\bar{Y}(k) - \bar{Y}(\infty) = C[x(k) - x(\infty)] = C e_x(k)$

Therefore, $Q = C^T C + q C_u^T C_u$ □

3. Multi-rate Short Seeking Control with Initial Value Adjustment for single-actuator HDDs

The demands for larger storage capacities and higher access speed continue to increase in the hard disk drive (HDD) industry. To meet these requirements, the servo bandwidth of the head positioning system must be increased to reject a wider range of disturbances such as disk flutter vibrations, spindle run-out, windage, and external vibration. Dual-stage actuation has been recognized as a promising candidate to expand the servo bandwidth. The dual-actuator disk file system consists of two actuators: coarse and fine actuators. The coarse actuator is of low bandwidth with a large operating range and it is used for coarse positioning; the fine actuator is of high bandwidth with a small operating range and it is used for fine positioning. The voice coil motor (VCM) and piezoelectric transducer (PZT) are the most popular coarse actuator and fine actuator, respectively.

Dual-stage actuators can improve both track-following and track-seeking performance. Many research efforts have been devoted to the design of dual-actuator servo system [7]-[12]. Several designs for dual stage track-following servos have been proposed, such as a decoupled type [7], a parallel type [8], a master-slave type [9], and a u-synthesis MIMO type [10]. Dual stage short seeking control can be achieved by a two-degree-of-freedom (TDOF) servo structure, in which both the feed-forward controller and reference trajectory need to be designed and implemented [11]-[12]. To save the real-time computation, we also propose a short-seeking control method based on multi-rate track following control and Initial Value Adjustment for dual-actuator HDDs. In this section, we will discuss the proposed method for dual-actuator HDDs in details.

3.1 Overall Control Structure for Dual-stage Short Seeking

Fig. 3 shows a schematic diagram of short seeking control with IVA for dual-actuator HDDs. P_{VCM} and P_{PZT} represent the dynamics of VCM (low bandwidth actuator) and PZT (high bandwidth actuator), respectively. In this study, the parallel track-following controllers are used to achieve high-accuracy track following, and C_1 and C_2 are, respectively, track following controllers for the VCM and PZT actuators. D and I are the decimator and the interpolator respectively. The proposed system has the following features:

- (1) The overall structure during seeking is a one-degree-of-freedom structure.
- (2) Reference input is set to be a step signal for short seek, i.e., $r(k)=r$ for $k \geq 0$, where r is the seeking distance. The output y is sampled with period T_f .
- (3) The feedback controllers are the same as the multi-rate track following controllers. The PZT controller C_2 is updated at the measurement sampling rate ($1/T_f$), while the VCM controller C_1 is updated m times slower than the measurement sampling rate with period $T_s=mT_f$. The multi-rate ratio m is an integer greater than 1.
- (4) Nonzero initial values are set to both controllers for short seeking.

Following similar procedure as single-stage short seeking , in the following sub-section 3.2, the multi-rate short seeking control problem is formulated as an optimization problem by converting the multi-rate control system depicted in Fig. 3 to an equivalent MIMO single-rate system. Then in sub-section 3.3, the optimal initial values of the controller for the equivalent MIMO system are sought to minimize the performance index. Design of performance index for dual-stage short-seeking is discussed in sub-section 3.4.

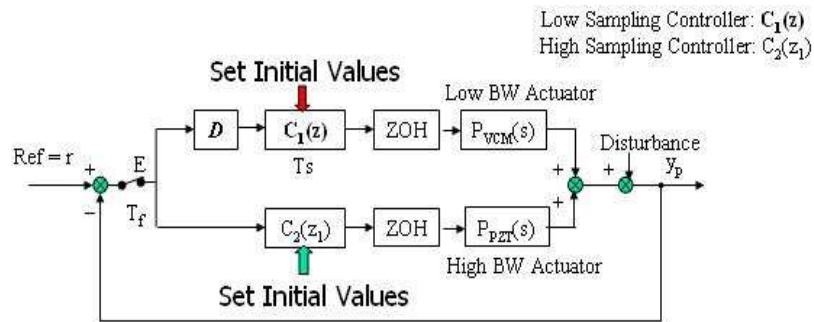


Fig.3 Schematic diagram of multi-rate short-peek control with IVA for dual-actuator HDDs

3.2 Representation of the Multi-rate Control System as a Single-rate system via Lifting

Assume that the dynamic models of VCM plant and PZT plant in continuous time are

$$\begin{aligned}\dot{x}_v(t) &= A_{01}x_v(t) + B_{01}u_v(t) \\ y_v(t) &= C_{01}x_v(t)\end{aligned}\quad (41)$$

$$\text{and} \quad \begin{aligned}\dot{x}_p(t) &= A_{02}x_p(t) + B_{02}u_p(t) \\ y_p(t) &= C_{02}x_p(t)\end{aligned}\quad (42)$$

where $x_v \in \mathfrak{R}^{n_v}$, u_v and y_v are the state vector, control input and output of VCM, and $x_p \in \mathfrak{R}^{n_p}$, u_p , y_p are the state vector, control input and output of PZT.

The discrete time equivalents of (41) and (42) with measurement sampling period T_f can be expressed by

$$\begin{aligned}x_v(k+1) &= A_1x_v(k) + B_1u_v(k) \\ y_v(k) &= C_1x_v(k)\end{aligned}\quad (43)$$

$$\text{and} \quad \begin{aligned}x_p(k+1) &= A_2x_p(k) + B_2u_p(k) \\ y_p(k) &= C_2x_p(k)\end{aligned}\quad (44)$$

where $x_v(k) = x_v(kT_f)$, $x_p(k) = x_p(kT_f)$, $A_1 \in \mathfrak{R}^{n_v^2}$, $B_1 \in \mathfrak{R}^{n_v}$, $C_1 \in \mathfrak{R}^{b_{01} \times n_v}$, $A_2 \in \mathfrak{R}^{n_p^2}$, $B_2 \in \mathfrak{R}^{n_p}$, $C_2 \in \mathfrak{R}^{b_{02} \times n_p}$

.Suppose track following controllers have already been designed for the dual-actuator HDD, and $C_1(z)$, $C_2(z)$ can be expressed in time domain as following:

$$\begin{aligned}x_{vc}(k+1) &= A_{c1}x_{vc}(k) + B_{c1}e(k) \\ u_v(k) &= C_{c1}x_{vc}(k) + D_{c1}e(k)\end{aligned}\quad (45)$$

$$\text{and} \quad \begin{aligned}x_{pc}(k+1) &= A_{c2}x_{pc}(k) + B_{c2}e(k) \\ u_p(k) &= C_{c2}x_{pc}(k) + D_{c2}e(k)\end{aligned}\quad (46)$$

where $x_{vc}(k) = x_{vc}(kT_f)$, $x_{pc}(k) = x_{pc}(kT_f)$,

$x_{vc} \in \mathfrak{R}^{n_{vc}}$, $A_{c1} \in \mathfrak{R}^{n_{vc}^2}$, $B_{c1} \in \mathfrak{R}^{n_{vc}}$, $C_{c1} \in \mathfrak{R}^{b_{c1} \times n_{vc}}$, $D_{c1} \in \mathfrak{R}$, $x_{pc} \in \mathfrak{R}^{n_{pc}}$, $A_{c2} \in \mathfrak{R}^{n_{pc}^2}$, $B_{c2} \in \mathfrak{R}^{n_{pc}}$, $C_{c2} \in \mathfrak{R}^{b_{c2} \times n_{pc}}$, $D_{c2} \in \mathfrak{R}$.

Referring to Fig. 3, C_1 is updated m times slower than C_2 . The control system in Fig. 3 cannot be described in the standard state-space form because it is a time-periodic system. Thus, we introduce a discrete-time lifting technique to describe the multi-rate system by an equivalent single-rate system, which may be accomplished in the following four steps.

STEP 1) The VCM controller (slow-rate controller) is transformed to an equivalent MIMO controller in the time domain with slow period T_s .

Lemma 3: Under the proposed multi-rate implementation scheme, the controller described by Eq.(45) can be represented by a MIMO system in time domain as following:

$$\begin{aligned} x_{vc}[k+1] &= A_{vc}x_{vc}[k] + B_{vc}\bar{e}[k] \\ \bar{U}_v[k] &= C_{vc}x_{vc}[k] + D_{vc}\bar{e}[k] \end{aligned} \quad (47)$$

where $x_{vc}[k] = x_{vc}(kT_s)$ (48)

$\bar{e}[k], \bar{U}_v[k]$ are the lifted position error signal and lifted control signal of VCM controller:

$$\bar{e}[k] = [e[k,0], e[k,1], \dots, e[k, m-1]]^T \quad \bar{U}_v[k] = [u_v[k,0], u_v[k,1], \dots, u_v[k, m-1]]^T \quad (49)$$

where $e[k, i] = e(kT_s + iT_f), u_v[k, i] = u_v(kT_s + iT_f)$

and $A_{vc} \in \mathfrak{R}^{n_{vc} \times n_{vc}}, B_{vc} \in \mathfrak{R}^{n_{vc} \times m}, C_{vc} \in \mathfrak{R}^{m \times n_{vc}}, D_{vc} \in \mathfrak{R}^{m \times m}$ are:

$$A_{vc} = A_{c1}^m, B_{vc} = \left[\sum_{j=0}^{m-1} A_{c1}^j B_{c1}, O \right], C_{vc} = \begin{bmatrix} C_{c1} \\ \vdots \\ C_{c1} \end{bmatrix}, D_{vc} = \begin{bmatrix} D_{c1} & O \\ \dots & \\ D_{c1} & O \end{bmatrix} \quad (50)$$

Proof:

Under the proposed multi-rate scheme, controller $C_l(z)$ is updated at slow rate ($1/T_s$), so the input to the controller is held constant during one slow period T_s , i.e.

$$e(kT_s) = e(kT_s + iT_f) \quad \text{for } i = 0, 1, \dots, m-1 \quad (51)$$

So,

$$\begin{aligned} x_{vc}[(k+1)T_s] &= x_{vc}(kT_s + mT_f) \\ &= A_{c1}x_{vc}(kT_s + (m-1)T_f) + B_{c1}e(kT_s + (m-1)T_f) \\ &= A_{c1}[A_{c1}x_{vc}(kT_s + (m-2)T_f) + B_{c1}e(kT_s + (m-2)T_f)] \\ &\quad + B_{c1}e(kT_s + (m-1)T_f) \end{aligned}$$

.....

$$\begin{aligned} &= A_{c1}^m x_{vc}(kT_s) + \sum_{i=0}^{m-1} A_{c1}^{m-1-i} B_{c1} e(kT_s + iT_f) \\ &= A_{c1}^m x_{vc}(kT_s) + \sum_{j=0}^{m-1} A_{c1}^j B_{c1} e(kT_s) \end{aligned} \quad (52)$$

Furthermore, from state equation (45),

$$u_v(kT_s) = C_{c1}x_{vc}(kT_s) + D_{c1}e(kT_s) \quad (53)$$

and by noting that the control signal is not updated during one slow period T_s , i.e. $u_v(kT_s + iT_f) =$

$u_v(kT_s)$, for $i=1,2,\dots, m-1$, we obtain

$$u(kT_s + iT_f) = C_{c1}x_{vc}(kT_s) + D_{c1}e(kT_s) \quad (54)$$

Combining Eqs. (52), (53), (54), and using (48) and (49), we can represent the controller as a time-invariant system with the slow update period T_s as described by Eq.(47). \square

STEP 2) The PZT controller (fast rate controller) is transformed to an equivalent MIMO controller in the time domain with slow period T_s .

By defining the lifted signal of $u_p(k)$ as:

$$\overline{U}_p[k] = [u_p[k,0], u_p[k,1], \dots, u_p[k,m-1]]^T \quad (55)$$

$$\text{where } u_p[k,i] = u_p(kT_s + iT_f), u_p(k) = u_p(kT_f)$$

and using (49), the PZT controller (46) can be converted to an equivalent MIMO controller given by

$$\begin{aligned} x_{pc}[k+1] &= A_{pc}x_{pc}[k] + B_{pc}\overline{e}[k] \\ \overline{U}_p[k] &= C_{pc}x_{pc}[k] + D_{pc}\overline{e}[k] \end{aligned} \quad (56)$$

$$\text{where } x_{pc}[k] = x_{pc}(kT_s),$$

$$A_{pc} = A_{c2}^m, B_{pc} = [A_{c2}^{m-1}B_{c2}, A_{c2}^{m-2}B_{c2}, \dots, B_{c2}], C_{pc} = [C_{c2}^T, (C_{c2}A_{c2})^T, \dots, (C_{c2}A_{c2}^{m-1})^T]^T$$

STEP 3) The VCM plant and PZT plant are expressed by equivalent MIMO plants in the time domain with the underlying slow period T_s .

By lifting the signals, $y_v(k)$ and $y_p(k)$, as

$$\overline{Y}_v[k] = [y_v[k,0], y_v[k,1], \dots, y_v[k,m-1]]^T, \quad \overline{Y}_p[k] = [y_p[k,0], y_p[k,1], \dots, y_p[k,m-1]]^T \quad (57)$$

$$\text{where } y_v[k,i] = y_v(kT_s + iT_f), y_p[k,i] = y_p(kT_s + iT_f)$$

and using (49) and (55), the VCM plant and PZT plant can be expressed by equivalent MIMO plants given by

$$\begin{aligned} x_v[k+1] &= A_v x_v[k] + B_v \overline{U}_v[k] \\ \overline{Y}_v[k] &= C_v x_v[k] + D_v \overline{U}_v[k] \end{aligned} \quad (58)$$

$$\text{and } \begin{aligned} x_p[k+1] &= A_p x_p[k] + B_p \overline{U}_p[k] \\ \overline{Y}_p[k] &= C_p x_p[k] + D_p \overline{U}_p[k] \end{aligned} \quad (59)$$

$$\text{where } x_v[k] = x_v(kT_s), x_p[k] = x_p(kT_s),$$

$$A_v = A_1^m, B_v = [A_1^{m-1}B_1, A_1^{m-2}B_1, \dots, B_1], C_v = [C_1^T, (C_1A_1)^T, \dots, (C_1A_1^{m-1})^T]^T$$

$$A_p = A_2^m, B_p = [A_2^{m-1}B_2, A_2^{m-2}B_2, \dots, B_2], C_p = [C_2^T, (C_2A_2)^T, \dots, (C_2A_2^{m-1})^T]^T$$

STEP 4) Combining the controllers and plants equations from STEPS 1, 2 and 3, we obtain an MIMO single-rate representation of the closed loop system in lifted form.

From the controllers equations, (47) and (56), and plants equations, (58) and (59), and referring to Fig. 5, we obtain the closed loop system:

$$\begin{aligned} x[k+1] &= Ax[k] + B\bar{r} \\ \bar{Y}[k] &= Cx[k] + D\bar{r} \end{aligned} \quad (60)$$

where $x[k] := [x_v[k]^T, x_p[k]^T, x_{vc}[k]^T, x_{pc}[k]^T]^T \in \mathfrak{R}^{n_v+n_p+n_{vc}+n_{pc}}$,
 $\bar{r} = [r, r, \dots, r]^T \in \mathfrak{R}^m$, $\bar{Y} = [y[k,0], y[k,1], \dots, y[k, m-1]]^T$

Matrices A , B , C and D can be computed from the system matrices in (47), (56), (58) and (59).

Now the multi-rate control system in Fig. 3 is converted to an equivalent MIMO single-rate system described by (60). The lifted system equivalent to the multi-rate short-seeking control system is shown in Fig. 4. Notice that the state of the closed loop system $x[k]$ can be separated into two parts: the states of two plants ($x_k[k]$) and the states of two controllers ($x_c[k]$):

$$x_k[k] := \begin{bmatrix} x_v[k] \\ x_p[k] \end{bmatrix}, \quad x_c[k] := \begin{bmatrix} x_{vc}[k] \\ x_{pc}[k] \end{bmatrix}.$$

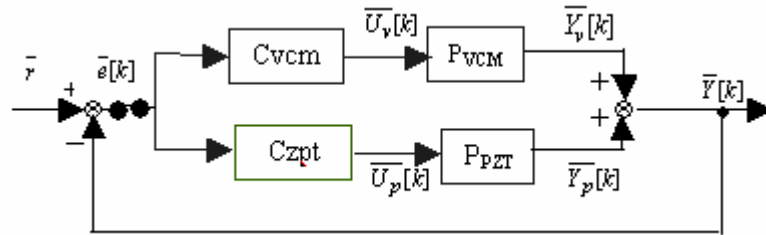


Fig. 4 Lifted system equivalent to the multi-rate short-seeking control system

The resulting closed loop system (60) is asymptotically stable because the multi-rate track following controller has been designed to stabilize the system. The error dynamics of the closed loop system is:

$$e_x[k+1] = Ae_x[k] \quad (61)$$

where $e_x[k] = x[k] - x[\infty]$, $x[\infty] = (I - A)^{-1}B\bar{r}$ (62)

3.2 Initial Value Adjustment of the Multi-rate Controllers for Dual-actuator HDDs

After the multi-rate control system is converted to an equivalent MIMO single-rate system, the initial value adjustment of the multi-rate controllers can be formulated as the following optimization problem.

Problem 2: Consider the multi-rate control system depicted in Fig. 3 or the equivalent MIMO single-rate system described by equation (60). Find the initial value of the controller $x_c[0]$ that minimizes performance index J :

$$J = \sum_{k=0}^{\infty} e_x[k]^T Q e_x[k], \text{ for } Q > 0 \quad (63)$$

where $e_x[k]$ is as defined in (62).

Theorem 2: The initial value of the controller $x_c[0]$ that minimizes performance index J is:

$$x_c[0] = K \bar{r} \quad (64)$$

$$\text{where } K = [P_{22}^{-1} P_{12}^T \quad I](I-A)^{-1} B \quad (65)$$

and P_{22}, P_{12} are obtained by solving the Lyapunov Eq.:

$$A^T P A - P = -Q, \quad P =: \begin{bmatrix} P_{11} & P_{12} \\ P_{12}^T & P_{22} \end{bmatrix} \quad (66)$$

The proof of Theorem 2 can be referred to that of Theorem 1.

From (64) and (65), we see that the initial value of the controller $x_c[0]$ is determined by \bar{r} , A , B and P . We further note that \bar{r} is determined by r and P is determined by Q and A . Thus, given, Q , r , A and B , the initial value of the controller $x_c[0]$ can be computed in advance. Compared with (27) and (28), it is noted that the initial value of the controller for dual-stage seeking has the same form as that of single-stage seeking, except that here $x_c[0]$ corresponds to the initial value of the two controllers. In the following section, we will discuss how Q may be designed for the dual-stage short seeking.

3.3 Design of Performance Index Function for Dual-stage Short Seeking

Design I- considering tracking error at sampling points

It is straightforward to evaluate the tracking error at sampling points and consider smoothness of the output and control input in the performance index: i.e.

$$J = \sum_{k=0}^{\infty} [e_y[k]^T e_y[k] + q_1 \dot{e}_y[k]^T \dot{e}_y[k]] + q_2 J_u \quad (69)$$

where $e_y[k] = \bar{Y}[k] - \bar{Y}[\infty]$, $\dot{e}_y[k] = [e_y[k+1] - e_y[k]]/T_s$,

$$J_u = \sum_{k=0}^{\infty} [\bar{U}[k] - \bar{U}[\infty]]^T [\bar{U}[k] - \bar{U}[\infty]], \quad \bar{U}[k] = [\bar{U}_v[k]^T, \bar{U}_p[k]^T]^T \quad (70)$$

q_1, q_2 are weighting factors.

Lemma 4: The performance index J in (69) can be transformed into the standard quadratic form:

$$J = \sum_{k=0}^{\infty} e_x[k]^T Q e_x[k]$$

where $Q = C^T C + q_1 C_d^T C_d + q_2 C_u^T C_u$,

$$C_d = C \frac{A-I}{T_s}, \quad C_u = (I + \begin{bmatrix} D_{vc} \\ D_{pc} \end{bmatrix} \begin{bmatrix} D_v & D_p \end{bmatrix}^{-1} \begin{bmatrix} -D_{vc} C_v, -D_{vc} C_p, C_{vc}, 0 \\ -D_{pc} C_v, -D_{pc} C_p, 0, C_{pc} \end{bmatrix}) \quad (71)$$

The proof is omitted here.

Design II- considering the inter-sampling behaviors

Design method I only evaluates the tracking error at the sampling instants. However, the plant is a continuous-time system, and it is natural to evaluate the continuous-time signals directly. Especially in dual-stage servos, inter-sampling ripple may take place if the second actuator has mechanical resonance modes at high frequencies beyond sampling frequency, which can be excited by the control input. To incorporate the inter-sampling errors, we modify J in (69) as follows:

$$J = \int_0^{\infty} [e_y(t)^2 + q_1 \dot{e}_y(t)^2] dt + q_2 J_u \quad (72)$$

where $e_y(t) = y(t) - y(\infty)$, J_u is as defined in (70).

To evaluate (72), the pieces of the continuous-time state $x_k(t)$ and $e_k(t)$ are introduced as:

$$\begin{aligned} x_k[k, i](v) &= x_k(kT_s + iT_f + v) \\ e_k[k, i](v) &= e_k(kT_s + iT_f + v) \end{aligned}, \quad v \in [0, T_f] \quad (73)$$

where $e_x(t) = x(t) - x(\infty) = [e_k(t)^T, e_c(t)^T]^T$

Lemma 5: $e_k[k, i](v)$ is a function of error-vector $e_x[k]$ as:

$$e_k[k, i](v) = He^{\hat{A}v} \bar{S}_i e_x[k], \quad v \in [0, T_f] \quad (74)$$

$$\text{where } \hat{A} = \begin{bmatrix} \hat{A}_{01} & O \\ O & \hat{A}_{02} \end{bmatrix}, \hat{A}_{01} = \begin{bmatrix} A_{01} & B_{01} \\ O & O \end{bmatrix}, \hat{A}_{02} = \begin{bmatrix} A_{02} & B_{02} \\ O & O \end{bmatrix}$$

$$\bar{S}_i = \begin{bmatrix} S_{vi} \\ S_{pi} \end{bmatrix} \times \begin{bmatrix} I_{n_v}, O \\ O_{n_p \times n_v}, I_{n_p}, O_{n_p \times (n_{vc} + n_{pc})} \\ C_u \end{bmatrix}, H = \begin{bmatrix} [I_{n_v}, O], O \\ O, [I_{n_p}, O] \end{bmatrix}$$

$$S_{vi} = \begin{bmatrix} A_1^i & O_{n_v \times n_p}, \sum_{j=0}^{i-1} A_1^j B_1, & O_{n_v \times m} \\ O_{1 \times n_v}, O_{1 \times n_p}, & A_{i+1} (1 \times m), & O_{1 \times m} \end{bmatrix}, A_{i+1} = [0, \dots, 0, \frac{1}{i}, \frac{0}{i+1}, \frac{0}{i+2}, \dots, 0]$$

$$S_{pi} = \begin{bmatrix} O_{n_p \times n_v} & A_2^i & O_{n_p \times m} & [A_2^{i-1} B_2, A_2^{i-2} B_2, \dots, B_2, 0, \dots, 0] \\ O_{1 \times n_v} & O_{1 \times n_p} & O_{1 \times m} & A_{i+1} (1 \times m) \end{bmatrix}$$

The proof is omitted here.

Noting that $y[k, i](v) = y_v[k, i](v) + y_p[k, i](v) = C_{01} x_v[k, i](v) + C_{02} x_p[k, i](v) = \hat{C}_0 x_k[k, i](v)$, $\hat{C}_0 = [C_{01} \ C_{02}]$

$$y[k, i](v) - y[\infty] = \hat{C}_0 e_k[k, i](v) \quad (75)$$

and using Lemma 5, we obtain

$$\begin{aligned} J_1 &= \int_0^{\infty} e_y(t)^2 dt = \sum_{k=0}^{\infty} \sum_{i=0}^{m-1} \sum_0^{T_f} \{ [y[k, i](v) - y[\infty]] dv \} \\ &= \sum_{k=0}^{\infty} \sum_{i=0}^{m-1} \sum_0^{T_f} \{ \int_0^{T_f} e_x^T[k, i](v) Q_c e_x[k, i](v) dv \} \\ &= \sum_{k=0}^{\infty} \sum_{i=0}^{m-1} \{ e_x^T[k] \bar{S}_i^{-T} \left(\int_0^{T_f} e^{\hat{A}v} (H^T Q_c H) e^{\hat{A}v} dv \right) \bar{S}_i e_x[k] \} \\ &= \sum_{k=0}^{\infty} \sum_{i=0}^{m-1} \{ e_x^T[k] \bar{S}_i^{-T} \hat{Q}_c \bar{S}_i e_x[k] \} = \sum_{k=0}^{\infty} e_x[k]^T Q_1 e_x[k] \end{aligned}$$

$$\text{where } Q_1 = \sum_{i=0}^{m-1} \bar{S}_i^{-T} \hat{Q}_c \bar{S}_i, \hat{Q}_c = \int_0^{T_f} e^{\hat{A}v} (H^T Q_c H) e^{\hat{A}v} dv, Q_c = \hat{C}_0^T \hat{C}_0$$

Thus, we conclude that the performance index J in (72) can also be transformed into the standard quadratic form as: $J = \sum_{k=0}^{\infty} e_x[k]^T Q e_x[k]$.

4. Simulations and Experiments

In this section, the proposed method is applied to a HDD and evaluated by simulations and experiments.

4.1 Experimental Setup

Figure 5(a) shows an experiment setup which includes a 3.5" HDD, a digital signal processor (TI TMS230C67X DSP), and a laser Doppler vibrometer for measuring the position of the read/write head. All the digital controllers are implemented on the DSP using C codes. The sampling rate is 50kHz, and the multi-rate ratio m is set to 2. Fig. 5(b) shows the HDD with voice coil motor (VCM) as a first-stage actuator and a piezo-electric transducer (PZT) as a second-stage actuator. The frequency responses of VCM and PZT plant models are shown in Fig. 5(c). Notice that they have resonance modes at high frequencies.

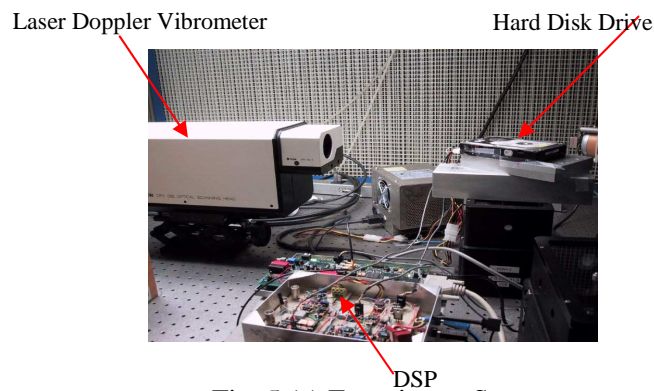


Fig. 5 (a) Experiment Setup

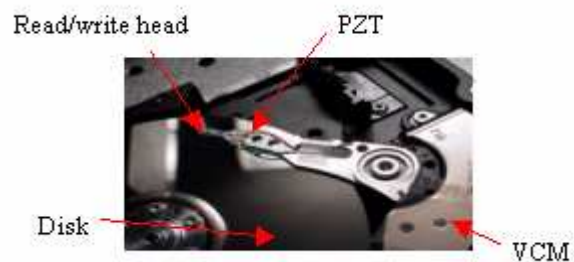
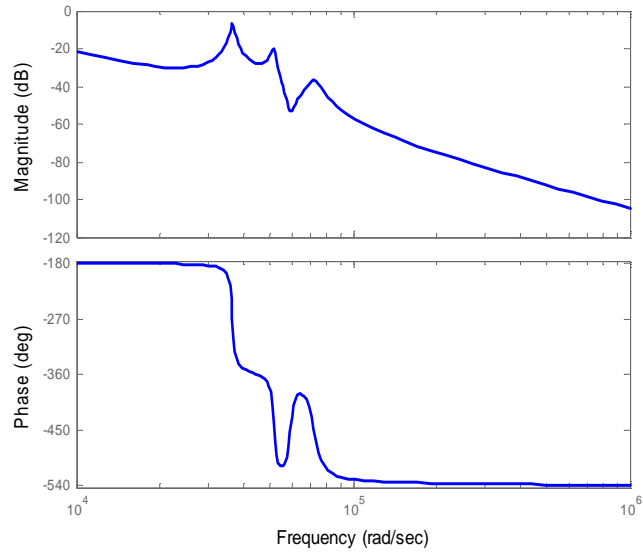


Fig. 5(b) Dual-actuator Hard Disk Drive



Error!

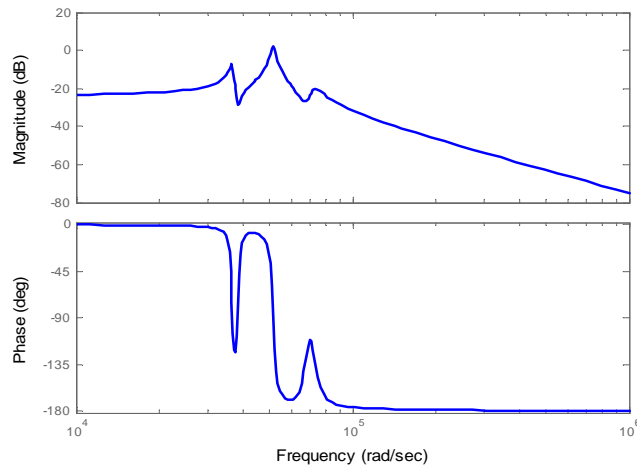


Fig. 5(c) Frequency responses of VCM and PZT plants

4.2 Simulations

4.2.1 Simulations Results - Short-Seeking with IVA for single-actuator HDDs

Here the simulations are performed on single-actuator HDD, which means we only use the first actuator VCM as plant. Simulation results of one-track seeking using proposed method for single-actuator HDD are shown in Fig. 6. The track pitch is $1 \mu\text{m}$. The solid line shows the

response of the proposed method and the dashed line shows the response of the output without initial value adjustment of the controller. From this figure, we can see that a fast and smooth response in short seeking can be achieved by initial value adjustment of the controller.

Figure 7 indicates how the transient characteristics may be shaped by different weighting factors q in the performance index. The upper figure shows the read/write head position and the lower figure shows the control input. We can observe from figure 7 that smaller weighting factor q ($q=400$) which allows for larger control input gives fast response but may lead to overshoot of head position, and larger weighting factor q ($q=40000$) which penalizes more on fluctuation of control input in the performance index gives smoother but much slower response. As a result, we can tune the weighting factor q to achieve desired step-responses taking into account both smoothness and settling time. Here we choose q to be 4000.

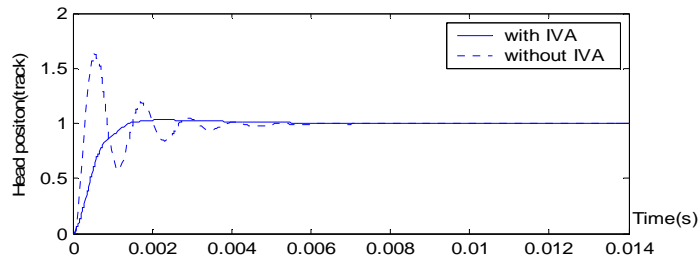


Fig. 6 Simulation result of 1-track seeking with/without IVA of the multi-rate controller for single-actuator HDDs

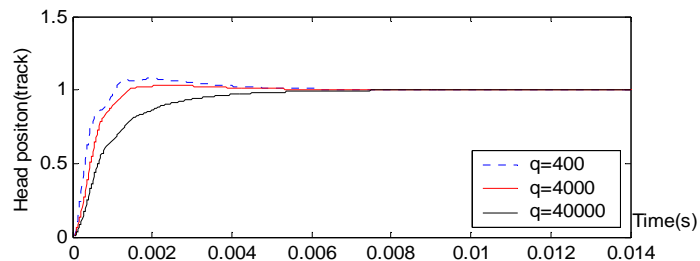


Fig. 7 (a) Simulation result of 1-track seek for different weighting factor q in performance index for single-actuator HDDs

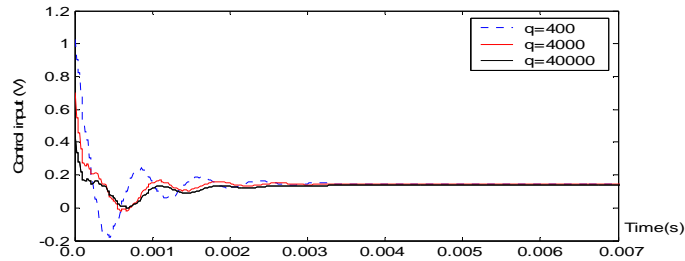


Fig. 7 (b): Control input of 1-track seeking for different weighting factor q in performance index for single-actuator HDDs

Figure 7(a): head position; figure 7(b): control input (for the first 7 ms), dotted line: $q=400$; light line: $q=4000$; dark line: $q=40000$

4.2.2 Simulation Results - Short-Seeking Control with IVA for Dual-actuator HDDs

Here the simulations are performed on dual-actuator HDD, which means we use both actuators.

Figure 8 shows the response of the output without initial value adjustment of the controllers for 1-track seeking. The dark line shows the head position, the light line and dotted line are VCM and PZT position respectively. Simulation results of 1-track seeking using proposed method are shown in Fig. 9. From Fig. 9, we can see that a fast and smooth response in short seeking can be achieved by initial value adjustment of the controllers.

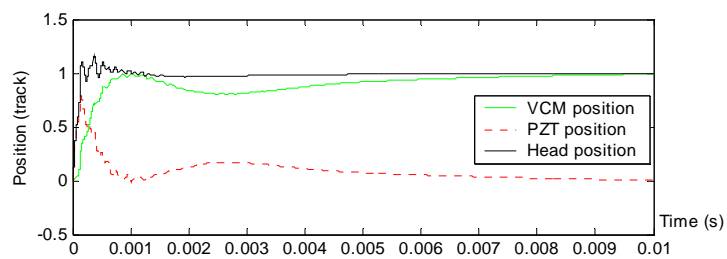
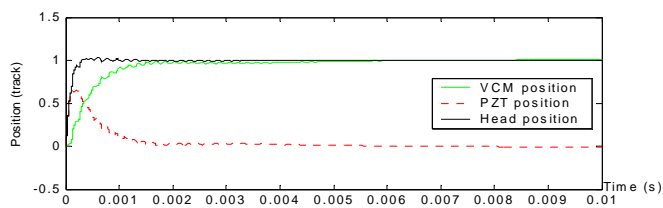
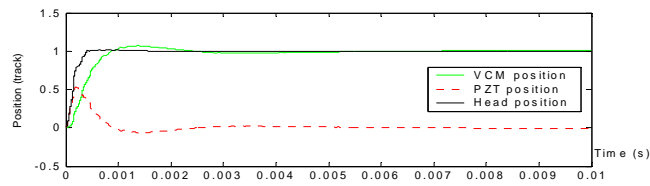


Fig. 8 1-track seeking without IVA for dual-actuator HDDs

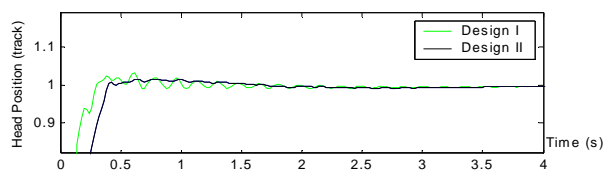
It could be noted from Fig. 9 that the dual-stage seeking control greatly improves the responses. It takes about 0.3 ms to move the head to the desired track so that the head can read or write data on the data track. The PZT actuator first moves towards the target track, and then returns to its stroke center to cancel out the movement of the VCM actuator after the head is on track. We can see PZT is within its stroke limit. Fig 9 (c) compares the performance of *Design I* and *Design II*, which confirms that inter-sampling ripple is decreased using *Design II*.



(a)



(b)



(c)

Fig. 9 1-track seeking with IVA for dual-actuator HDDs

(a) *Design I*; (b) *Design II*;

(c) Head position around target track, dark line: *Design II*; light line: *Design I*.

4.3 Experiments

4.3.1 Experimental Results - Short-seeking control with IVA for single-actuator HDDs

The experimental result of 1-track seeking using the proposed method ($q=4000$) for single-actuator HDD is shown in Fig. 10. We can see that the experiment result matches the simulation results very well, and performance is very good. Figure 11 is a zoom-in version of Fig. 10.

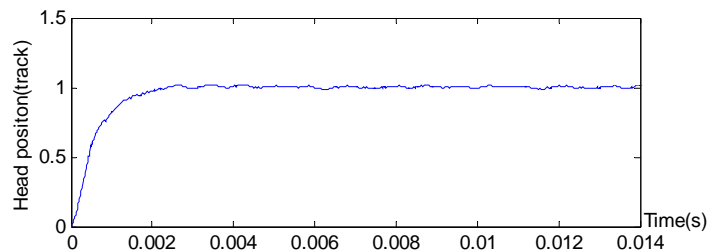


Fig. 10 Experimental result of 1-track seek using the proposed method for single-actuator HDD

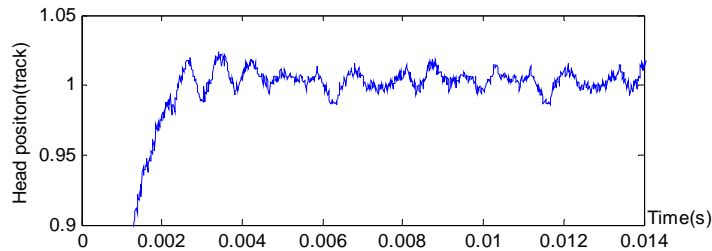


Fig. 11 Experimental result of 1-track seeking using the proposed method for single-actuator HDD
(zoom-in version of Fig. 10)

4.3.2 Experimental Results -Short-seeking with IVA for dual-actuator HDDs

The experimental result of 1-track seeking using the proposed method for dual-actuator HDD is shown in Fig. 12. Fig. 13 is a zoom-in version of Fig. 12. We can see the performance is excellent: 10% settling time is only 0.3 ms, and 3σ of PES after settling is only 1.9% of the track pitch.

Table I summarizes the experimental results for both single-actuator seeking and dual-actuator seeking. We can see the performance of both cases are very good, and under proposed scheme, dual-actuator seeking outperforms single-actuator seeking by reducing settling time by about 76.2% and decreasing 3σ of PES by about 26.9%.

Error!

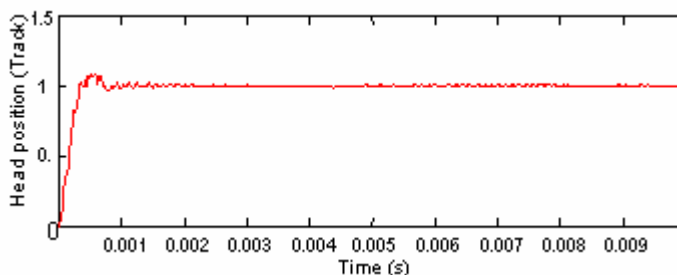


Fig. 12 Experimental result of 1-track seek using the proposed method for dual-actuator HDDs

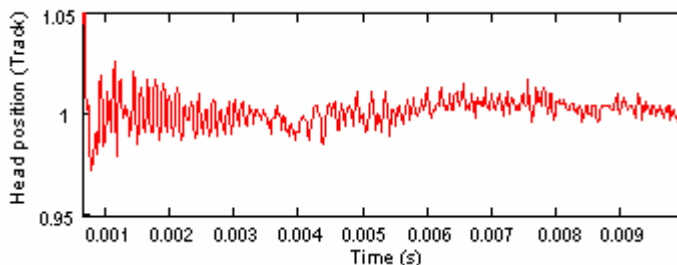


Fig. 13 Experimental result of 1-track seek using the proposed method dual-actuator HDDs

(zoom-in version of Fig. 12)

TABLE I

Short-seeking performance using the proposed method
(Experimental Results)

| Experiment Results | Single actuator seek | Dual actuator seek |
|---|----------------------|--------------------|
| 10% Settling Time (ms) | 1.26 | 0.30 |
| 3σ of PES after settling (Track) | 0.026 | 0.019 |

5 Conclusions

In this report, we have proposed a short seeking control based on multi-rate track-following controller and initial value adjustment for reduced real time computation. The multi-rate short seeking control problem was formulated as an optimization problem by converting the multi-rate control system to an equivalent MIMO single-rate system and finding the optimal initial values of the controller for the equivalent MIMO system.

The proposed method has been applied to both single-actuator HDDs and dual-actuator HDDs. By incorporating the inter-sampling error and the smoothness of the control input and output in the performance index, initial value adjustment of the feedback controllers can achieve smooth and fast short seeking in both cases.

Simulation and experimental results confirmed that an excellent short-seeking performance can be achieved with a small amount of real time computation using the proposed methods, and that under proposed scheme, the dual-actuator system has better short seek performance than the single-actuator seek system.

Acknowledgement

This work was conducted at the Computer Mechanics Laboratory of the University of California, Berkeley.

References

- [1] S-C. Wu and M. Tomizuka, "Multi-rate digital control with interlacing and its application to hard disk drive servo," *Proceedings of the 2003 American Control Conference*, Denver, June 4-6, pp. 4347-4352.
- [2] S. Shishida, T. Yamaguchi, H. Hirai, *et al.*, "Fast head positioning method of magnetic disk drives," *IEEE Trans. Magnetics*, 1993, 29(6), 4045–4047.
- [3] L. Yi and M. Tomizuka, "Two-degree-of-freedom control with robust feedback control for hard disk servo systems," *IEEE/ASME Trans. on Mechatronics*, vol. 4, no. 1, pp. 17-24, 1999.
- [4] H. Fujimoto, Y. Hori, T. Yamaguchi, S. Nakagawa, "Seeking control of hard disk drive by perfect tracking using multirate sampling control," *Transactions of the Institute of Electrical Engineers Japan, Part D*, vol.120-D, no.10, Oct. 2000, pp.1157-1164.
- [5] J. Ishikawa, Y. Yanagita, T. Hattori, M. Hashimoto, "Head positioning control for low sampling rate systems based on two degree-of-freedom control," *IEEE Transactions on Magnetics*, vol.32, no.3, May 1996, pp.1787-1792.
- [6] M. Hirata and M. Tomizuka, "Multi-Rate Short Track-Seeking Control of Hard Disk Drives for Computation Saving," *Proceedings of the 2003 IEEE Conference on Decision and Control*, Maui, December 2003 (Paper ThA11.2).
- [7] K. Mori *et al.*, "A dual-stage magnetic disk drive actuator using a piezoelectric drive for a high track density," *IEEE Trans. Magn.*, vol. 27, no. 6, pp. 5298–5300, 1991.
- [8] T. Semba *et al.*, "Dual-stage servo controller for HDD using MEMS microactuator," *IEEE Trans. Magn.*, vol.35, no.5, pp.2271–73, 1999.
- [9] S. Koganezawa, Y. Uematsu, and T. Yamada, "Dual-stage actuator system for magnetic disk drives using a shear mode piezoelectric microactuator," *IEEE Trans. on Magnetics*, vol.35, no.2, Mar. 1999.
- [10] D. Hernandez, S. Park, R. Horowitz, and A. K. Packard, "Dual-stage track-following servo design for hard disk drives," *Proc. Amer. Control Conf.*, 1999, pp. 4116–4121.
- [11] M. Kobayashi and R. Horowitz, "Track Seek Control for Hard Disk Drive Dual-Stage Servo Systems", in *Transaction on Magnetics*, Vol. 37, No. 2, March 2001.

- [12] J. Ding, and M. Federico and M. Tomizuka, "Short Seeking Control with Minimum Jerk Trajectories for Dual Actuator Hard Disk Drive Systems," *Proc. American Control Conf.*, Boston, 2004